

# Optical measurement of rates of dissipation of temperature variance due to oceanic turbulence

D. J. Bogucki<sup>1\*</sup>, J. A. Domaradzki<sup>2</sup>, C. Anderson<sup>3</sup>, H. W. Wijesekera<sup>4</sup>,  
J. R. V. Zaneveld<sup>5</sup> and C. Moore<sup>5</sup>

<sup>1</sup> RSMAS/University of Miami Division of Applied Marine Physics 4600 Rickenbacker Cswy  
Miami, FL 33149-1098

\* [Corresponding author: dbogucki@rsmas.miami.edu](mailto:dbogucki@rsmas.miami.edu)

<sup>2</sup> Aerospace and Mechanical Engineering, University of Southern California, Los Angeles, CA  
90089-1191

<sup>3</sup> SpectraScan Corp., Inc., 909 Electric Avenue, Suite 304, Seal Beach, CA 90740

<sup>4</sup> College of Oceanic and Atmospheric Sciences, Oregon State University, Corvallis, OR  
97331-5503

<sup>5</sup> WET Labs, Inc., 620 Applegate St., Philomath, OR 97370

**Abstract:** Inhomogeneities in the refractive index induced by temperature fluctuations in turbulent flows have the effect of scattering light in near-forward angles. We have developed a method that extracts the rate of Temperature Variance Dissipation (TVD) and its spectrum from the properties of light scattering and have built an instrument - Optical Turbulence Sensor (OTS) - that implements the method. OTS uses a linear wavefront sensing Hartmann array and allows for nearly instantaneous measurements of temperature variance in turbulent flows. The instrument has been tested in an *in situ* experiment carried out from a drifting vessel at a site off the coast of Newport, Oregon. Here we compare the temperature variance measured by OTS and its spectra with both theoretical predictions and with spectra obtained from a fast thermistor sensor.

© 2007 Optical Society of America

**OCIS codes:** (010.7350) Wave-front sensing, (010.7060) Turbulence

---

## References and links

1. R. V. Ozmidov, "On the turbulent exchange in a stably stratified ocean." *Izvestiya, Atmospheric and Oceanic Physics* **1**, 493–497 (1965).
2. W. H. Wells, "Theory of Small-angle Scattering," (Advisory Group for Aerospace Research and Development, NATO, 92 Neuilly-Sur-Seine, France, 1973).
3. D. Bogucki, J. A. Domaradzki, D. Stramski, and J. R. V. Zaneveld, "Comparison of nearforward scattering on turbulence and particles," *Applied Optics* **37**, 4669–4677 (1998).
4. D. J. Bogucki, J. A. Domaradzki, R. E. Ecke, and R. C. Truman, "Light scattering on oceanic turbulence," *Appl. Opt.* **43**, 5662–5676 (2004).
5. D. J. Bogucki, J. A. Domaradzki, R. E. Ecke, C. R. Truman, and J. R. V. Zaneveld, "Near-forward light scattering on oceanic turbulence and particulates: an experimental comparison," vol. SPIE, *Ocean Optics XIV* (1998).
6. R. G. Lueck, D. Huang, D. Newman, and J. Box, "Turbulence Measurement with a Moored Instrument," *Journal of Atmospheric and Oceanic Technology* **14**, 143–161 (1997).

7. M. C. Gregg, "Uncertainties and Limitations in Measuring  $\varepsilon$  and  $\chi$ ." *Journal of Atmospheric and Oceanic Technology* **16**, 1484–1490 (1998).
8. V. I. Tatarski, *Wave Propagation in Turbulent Media* (McGraw-Hill, New York, 1961).
9. V. I. Tatarski, *The effects of the turbulent atmosphere on the wave propagation* (Israel program for Scientific Translation, Jerusalem, 1971).
10. A. S. Monin and A. M. Yaglom, *Statistical Fluid Mechanics: Mechanics of Turbulence* (The MIT press, 1981).
11. D. Bogucki, A. Domaradzki, and P. K. Yeung, "Direct numerical simulations of passive scalars with  $Pr > 1$  advected by turbulent flow," *J. Fluid Mech.* **343**, 111–130 (1997).
12. D. Bogucki and J. Domaradzki, "Numerical study of light scattering by a boundary-layer flow," *Appl. Opt.* **44**, 5286–5291 (2005).

## 1. Introduction

The fluxes of heat, salt, nutrients, oxygen, etc. are of primary importance in applications as diverse as modeling of ocean circulation, primary productivity, pollutant dispersal, particle and sediment transport. Typically, estimates of turbulent fluxes in the ocean are obtained from assumed relations between these fluxes and the rates of turbulent kinetic energy dissipation (TKED) and of temperature variance dissipation (TVD). Typical oceanic flows are turbulent and are characterized by a wide range of coexisting scales of motion. For example, temperature within an oceanic eddy varies on scales between  $O(10) m$  and  $1 mm$  [1]. For some time [2], the optical oceanography community has theoretically postulated the effect of turbulence on light propagation in the ocean. Turbulent fluctuations of passive scalars (such as temperature and salinity) in water cause fluctuations in the density of the fluid, and hence in its refractive index, affecting light propagation. Inhomogeneities in the refractive index can be attributed mainly to the temperature field [3].

Recent theoretical research on the importance of scattering on turbulence [3] aimed to quantify its effect relative to scattering on particles. Turbulent scattering was typically found to dominate at small angles, less than  $0.1^\circ$  ( $1.7 \cdot 10^{-3} rad$ ), and for propagation distances of  $\simeq 0.3 m$ . However, experimental oceanic studies of the interaction between light and turbulence have been rare, in large part due to the complexity of appropriate experiments and to the difficulty of making angular measurements of scattered light at small angles in the presence of the unscattered light beam.

Recent laboratory measurements of near-forward scattering (range of  $10^{-7}$  to  $10^{-3} rad$ ) of the light beam on turbulent flow show that under energetic oceanographic conditions, the total scattering coefficient can be larger than that of particulates and that the turbulent inhomogeneities of fluid flow have the effect of scattering light in near-forward angles, thus providing an opportunity to use optics to quantify turbulence [4].

In this paper we present results from the in situ optical measurements of turbulent quantities using a packaged version of the laboratory setup developed previously and described in Bogucki et. al. [5, 4], concurrent with a fast-response thermistor and additional turbulent microstructure sensor package, described in more detail in, for example [6, 7]. In ocean TVD ranges from  $10^{-2} \text{ }^\circ C^2/s$  a few meters below the surface to  $10^{-10} \text{ }^\circ C^2/s$  in the deep ocean. TKED can vary from  $10^{-4} m^2/s^3$  in the fairly energetic upper layer to  $10^{-11} m^2/s^3$  in mid-water column [3]. In the current configuration OTS was designed to measure TVD in the range  $10^{-9}$  to  $10^{-1} \text{ }^\circ C^2/s$  and TKED within  $10^{-10}$  to  $10^{-4} m^2/s^3$  range making it most suitable to the upper ocean measurements. Combining the optical measurement with appropriate processing allows nearly instantaneous estimation of spectra of temperature variance and thus of the rates of temperature variance dissipation.

## 2. Principles of the optical determination of the temperature variance spectrum

A scalar, near-forward approximation to Maxwell's equations for a short propagation path, such that  $L = 0.3 \text{ m}$ , can be expressed in terms of the function  $\psi$ , which represents the complex amplitude of a 2-D light front propagating in the  $z$  direction over the pathlength  $L$  [8]:

$$\psi(x, y) = A_0(x, y) \exp\left(\frac{2\pi i}{\lambda} \int_0^L n(x, y, z') dz'\right), \quad (1)$$

where:  $A_0$  is the initial value of  $\psi(x, y)$  at  $z = 0$  (a constant, for a plane wave);  $\lambda$  is the light wavelength, and  $n(x, y, z)$  is a small deviation of the local refractive index from its mean value. The exponent in Eq. (1), the function  $\int_0^L n(x, y, z') dz'$ , depends on the refractive index of the medium where light propagates. This expression (for the given  $x$  and  $y$ ) gives the phase of the light after it has propagated over the distance  $L$ :  $\Gamma(x, y) = \int_0^L n(x, y, z) dz$ . The vector normal to  $\Gamma(x, y)$

$$\mathbf{N} = \left[ \frac{\partial \Gamma}{\partial x}, \frac{\partial \Gamma}{\partial y}, 1 \right], \quad (2)$$

is parallel to the direction of the scattered ray. The value of the medium-dependent scattering angle  $\alpha(x, y)$  ( $\alpha$  is sometimes called angle-of-arrival) over the pathlength  $L$  can thus be obtained as:

$$\alpha(x, y) = \left\{ \left( \frac{\partial \Gamma}{\partial x} \right)^2 + \left( \frac{\partial \Gamma}{\partial y} \right)^2 \right\}^{1/2}, \quad (3)$$

The physical principle of optical turbulence measurement relies on the fact that turbulent fluctuations of scalars such as temperature or salinity in water cause fluctuations in the density of the fluid, and hence in its refractive index. In the ocean the inhomogeneities in the refractive index are frequently dominated by fluctuations in the temperature field [3]. Assuming that the temperature variations dominate the small scales refractive index variations, the small scale refractive index is a function of a position through the water temperature only, i.e.:  $n(x, y, z) = n(T[x, y, z])$ . Therefore, equations (1) -(3) constitute an implicit relation between temperature fluctuations and scattering angle. The optical measurement approach involves measuring the light scattering angle after it propagates a fixed distance. This path-integrated effect of fluctuations in the refractive index can be used to obtain the wavenumber spectra of temperature field as proposed in [9]. Specifically, the 2D spatial autocorrelation of the scattered ray angle,  $B(\rho)$ , is used and then related to the 3-dimensional Fourier spectrum of temperature fluctuations,  $E_T(k)$  ( $k$  - is the spatial wavenumber  $\propto 1/\text{lengthscale}$ ). The spatial autocorrelation of the scattered ray angle is:

$$B(\rho) = \int_D \alpha(\rho') \alpha(\rho - \rho') d\rho' \quad (4)$$

where the radial distance  $\rho$  is defined as:  $\rho = (x^2 + y^2)^{1/2}$ , and the domain  $D$  is a plane which is perpendicular to the propagation axis  $Oz$ . For measurements of light scattering on oceanic turbulence and propagation over pathlengths of  $L = 0.3 \text{ m}$ ,  $D$  is effectively truncated to a fraction of the entire plane because the majority of the turbulence scattered light is within a very narrow cone within  $0.1^\circ$  ( $1.7 \cdot 10^{-3} \text{ rad}$ ) of the original beam direction [3]. The exact procedure for calculating the temperature spectra from the autocorrelation of the angles is outlined in [10] (Volume II, Chapter 9) and similarly in [9] (Chapter 3). The main stages involved are: writing the light wavefront phase in terms of the angle-of-arrival of the wavefront across the receiving aperture, then taking the Fourier transform of the angular autocorrelation, and finally, inverting it to obtain the temperature spectrum  $E_T(k)$ . This approach is based on the following relation

between direct measurements of the correlation function of fluctuations in the angle-of-arrival,  $B(\rho)$ , and the temperature variance spectra ([9], Eq. (42), p. 189):

$$M^2 \int_0^\infty k J_0(k\rho) E_T(k) dk = \frac{1}{\rho} B(\rho), \quad (5)$$

where constant  $M = G \langle dn/dT \rangle$  and the  $\langle dn/dT \rangle$  is the coefficient in the Taylor expansion (typically for oceanic conditions of around  $10^{-4} \text{ }^\circ\text{C}^{-1}$ ) of water refractive index  $n(T)$  at a given water temperature  $T$  and  $G$  is an OTS geometrical constant related to used CCD dimensions. This relationship, Eq. (5), can be inverted via the Hankel transform to obtain the temperature spectra  $E_T(k)$ :

$$E_T(k) = \frac{1}{M^2} \int_0^\infty J_0(k\rho) B(\rho) d\rho. \quad (6)$$

The physical interpretation of  $E_T(k)$  is that the temperature variance for length scales between  $k$  and  $k + dk$  is proportional to  $E_T dk$ . In general the spectrum  $E_T(k)$  depends parametrically on molecular properties of water, i.e. the kinematic viscosity  $\nu$  and the thermal diffusivity  $\kappa$ , as well as on the turbulent kinetic energy dissipation rate and the rate of temperature variance dissipation. The TVD rate can be directly found from its definition as a weighted integral of the temperature spectrum i.e.:

$$\chi = 2\kappa \int_0^\infty E_T(k) k^2 dk. \quad (7)$$

where the quantity  $E_T(k)k^2$  is the temperature dissipation spectrum [11].

### 3. Optical Turbulence Sensor

A photograph of the OTS prototype (panel A) and its schematics (panel B) are shown in Fig. 1. A functional description follows below. The light source was a 670 nm laser diode. The beam was expanded, collimated and then propagated through the turbulent flow across the path length  $L = 0.3 \text{ m}$  exposed to the oceanic water. After interacting with the turbulent flow, the light beam passes through a linear wavefront sensing Hartmann array, consisting of 110 lenslets for a total length of 5 cm, and a line scan CCD. The lenslet spots are imaged onto the CCD linear 8k pixel array. The CCD light intensity data, consisting mostly of 110 bright spots, were then low-passed filtered to remove the effect of high frequency noise - oceanic particles. The 'cleaned up' linear Hartmann array data was then transformed [4] into equivalent 2D spatial autocorrelation function and then converted into the temperature spectra  $E_T(k)$ . The Hartmann array was capable of measuring scattering angles from  $0.3 \mu \text{ rad}$  to a few *milirad* and operated at the speed of a 10000 CCD readings per second during a measuring interval.

### 4. Turbulence measurements using microstructure sensing package

The oceanographic, 'reference' microstructure sensing package carries a capillary micro-conductivity sensor, a fast-response thermistor (FP10), and a Doppler current meter- ADCP, which measures in situ flow speed in the vicinity of the package. By combining local T-S properties, the rate of temperature variance dissipation was computed directly from microscale conductivity fluctuations (e.g., Dillon et al., 2003). We also collected differentiated temperature fluctuations from FP10, but during drifting-ship measurements, the thermistor response was not fast enough to resolve the dissipation range of temperature gradient spectrum (e.g., Dillon and Caldwell, 1980). The microscale conductivity sensor collected data at a rate of 2048 Hz. The fast response thermistor, FP10, pressure sensor collected data with 256 Hz rate.

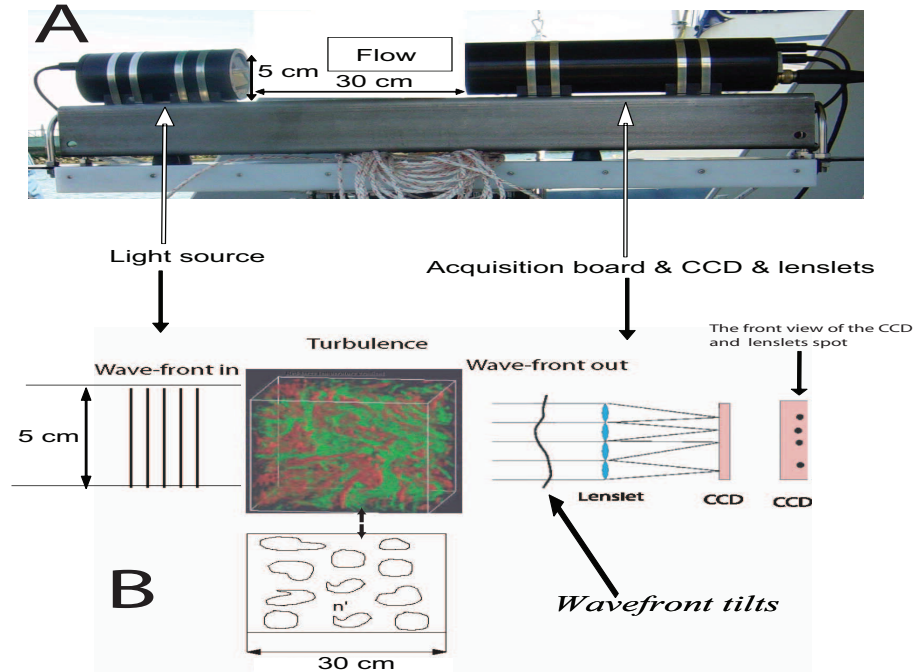


Fig. 1. Optical Turbulence Sensor - (A) Photograph of the developed and sea tested sensor. (B) Schematic representation of the various OTS parts. The light source is on the left hand side. The right hand side contains the receiving unit. Examples of displaced spots (only 4 of 110 available in OTS) produced by lenslets are presented on the right hand side of Figure (B). The light source and the acquisition board with CCD are enclosed in a hermetic enclosure.

## 5. Results

Microstructure data sets to test the performance of the Optical Turbulence Sensor (OTS) were collected off the coast of Newport, OR, using a 54-foot long vessel, R/V Elakha. The microstructure sensing package was mounted closely to the OTS sensor. The measurements were carried out by lowering the sensing package (probes, fast thermistors, ADCP and the OTS) just behind the fantail of R/V Elakha. The sensing package was lowered in the ship's wake, exposing the sensors to the ship generated wake and ambient turbulence. All sensors sensed approximately same part of the water column. In the previous theoretical investigation [12] the OTS generated turbulence has been found to be negligible. The local water depth varied between 49 m initially till the ship drifted to a water depth of 38.5 m. The time series were collected during a period of 1.8 hours. In the following we compare the TVD rates from the OTS and the microstructure package by looking at the time series measurements at three different depths,  $\approx 3$  m (between 10.2 and 11.00 local time),  $\approx 2$  m (between 11 and 11.8 local time), and  $\approx 6.5$  m (between 11.8 and 12.2 local time), to capture variability in the dissipation rates.

The OTS acquired each individual spectrum in 5 to 7  $\mu\text{sec}$ . The spectral ensemble typically became stable after approximately 50 realizations, corresponding to an averaging time of 5 msec (this time includes the overhead time for the camera-acquisition system). For this paper we averaged all OTS spectra down to 2 sec to enable comparison of TVD rates with those derived from the fast thermistor data, which yields a data point every 2 seconds. An example of 2-sec OTS temperature variance and dissipation spectra are presented in the Fig 2. Figure 3

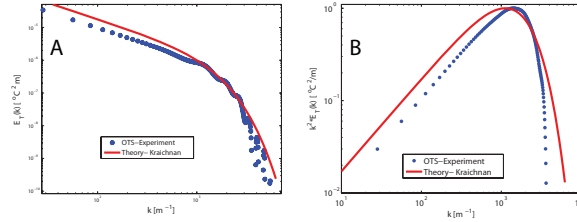


Fig. 2. Example of temperature spectrum  $E_T(k)$  - panel (A) and dissipation spectrum  $k^2 E_T(k)$  - panel (B) measured by OTS (2 sec ensemble), compared to theoretical prediction for turbulent flow [11].

shows the time series of  $\chi$  measured by OTS and compared to that obtained from the thermistor/conductivity measurements. The two measurements are consistent although OTS provides a much narrower  $\chi$  variance. We hypothesize that the major reason for the variance differences lies in the different physical nature of these two measurement. Traditional microstructure measurements use the 'Frozen Field' assumption and thus require very accurate mean current speed,  $U_x$ , to convert the time derivatives to spatial ones (i.e.  $\partial/\partial x = 1/U_x \cdot \partial/\partial t$ ). The OTS measurement does not rely on the existence of the current speed. The OTS measurement yields an instantaneous estimate of angular autocorrelation and resulting temperature spectra  $E_T(k)$  as long as they remain unchanged during the measurement time - 5 to 7  $\mu sec$ .

The mean flow  $U_x$  varied during the experiment between a few  $m/s$  down to few tens of  $cm/s$  and  $U_x$  was highly variable over the integration time. We estimate that this factor alone increases the variance of  $\chi$  derived from the time series of thermistor/conductivity by at least a factor of 4, thus contributing to much larger variance of  $\chi$  in Fig. 3. In addition the OTS variance is more stable because each OTS data point (corresponding to the 2 sec long time series of thermistor/conductivity measurement) consists of 2000 values averaged to one number. The OTS needs more in situ testing in a variety of oceanographic conditions to fully address similarities and differences to existing oceanographic turbulence measurements methods.

## 6. Conclusions

We have shown that the rates of temperature variance dissipation can be determined using optical techniques in the prototype configuration known as OTS. By comparing measurements of  $\chi$  from the OTS with those from a classical microstructure instrument, we conclude that the OTS provides consistent results. The main difference is the lower variance of the rate of temperature variance dissipation measured by the OTS. The highly variable mean flow affects the microstructure measurements but has no effect on the OTS results.

## Acknowledgments

This work was supported by ONR SBIR Phase II grant to SpectraScan Corp. We thank Dr. Iturriaga and the crew of R/V Elakha for help during the sea tests.

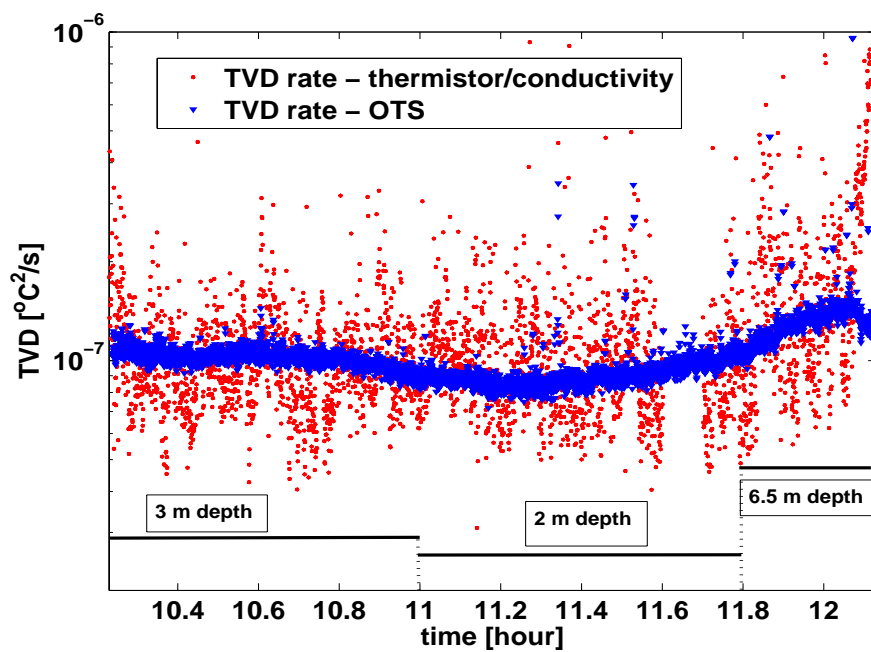


Fig. 3. The 2 hour time series of  $\chi$  measured by OTS and the thermistor at each measurement depth.